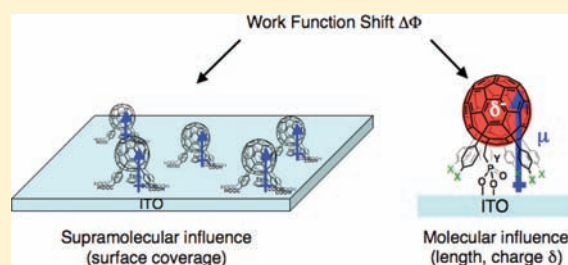# Molecular and Supramolecular Control of the Work Function of an Inorganic Electrode with Self-Assembled Monolayer of Umbrella-Shaped Fullerene Derivatives

Sebastian Lacher, Yutaka Matsuo, and Eiichi Nakamura*

Department of Chemistry, The University of Tokyo, 7-3-1 Hongo, Bunkyo-ku, Tokyo 113-0033, Japan

S *Supporting Information*

ABSTRACT: The surface properties of inorganic substrates can be altered by coating with organic molecules, which may result in the improvement of the properties suitable for electronic or biological applications. This article reports a systematic experimental study on the influence of the molecular and supramolecular properties of umbrella-shaped penta(organo)[60]fullerene derivatives, and on the work function and the water contact angle of indium—tin oxide (ITO) and gold surfaces. We could relate these macroscopic characteristics to single-molecular level properties, such as ionization potential and molecular dipole. The results led us to conclude that the formation of a SAM of a polar compound generates an electronic field through intermolecular interaction of the molecular charges, and this field makes the overall dipole of the SAM much smaller than the one expected from the simple sum of the dipoles of all molecules in the SAM. This effect, which was called depolarization and previously discussed theoretically, is now quantitatively probed by experiments. The important physical properties in surface science such as work function, ionization potential, and water contact angles have been mutually correlated at the level of molecular structures and molecular orientations on the substrate surface. We also found that the SAMs on ITO and gold operate under the same principle except that the "push-back" effect operates specifically for gold. The study also illustrates the ability of the photoelectron yield spectroscopy technique to rapidly measure the work function of a SAM-covered substrate and the ionization potential value of a molecule on the surface.

■ INTRODUCTION

Surface modification is crucial to achieve high performance of organic electronic devices, such as organic photovoltaics, organic light-emitting diodes,[1] and chemical or biological sensing devices.[2,3] The coating of inorganic substrates such as metal oxides and metals with self-assembled monolayers (SAMs) or thin films of organic molecules effectively alters the work function (WF) and the surface energy of electrodes. Such a coating can tune the WF of an electrode, for example, indium—tin oxide (ITO), over more than 1 eV (vide infra), because the dipoles of the molecules modify the intrinsic surface dipole of the substrate.

Theoretical models have been proposed to quantify the influence of a SAM on the WF shift, $\Delta\Phi$, of an electrode. The Helmholtz equation (eq 1) represents a basic theory in which the SAM is treated as a continuous dipole sheet composed of molecules standing on a flat electrode surface. If n is the area density of dipoles on the surface, ε_0 is the vacuum permittivity, e is the elementary charge $(1.6022 \times 10^{-19}$ C$)$, μ is the dipole moment, and θ is the average tilt angle of the dipole with respect to the surface normal:

$$\Delta\Phi(n) = en\mu(n)\cos\theta/\varepsilon_0 \tag{1}$$

The dependence of the molecular dipole on the surface coverage was further refined by Topping's model in 1927. This

theory took into account the electronic field generated by intermolecular interaction of the charges of the molecules and proposed that this field makes the overall dipoles of the SAM much weaker than the one expected from the simple sum of the dipole of all molecules in the SAM (depolarization effect).[4] In fact, the depolarization effect was found qualitatively to become a dominant factor in the case of densely packed SAMs, especially for molecules with high polarizability and large dipoles.[5]

Despite the long-standing interest in molecular dipoles and the WF, quantitative experimental studies on the depolarization effect have been scarce[6,7] for several fundamental reasons. For instance, an ideal SAM on an electrode that is necessary for such quantitative studies is difficult to make, especially for low surface coverage,[8] and the determination of its molecular and supramolecular structures at molecular precision is very difficult, too.[9] The molecules often form multilayers, aggregates, islands, and domains, and therefore the surface coverage, molecular dipole, angle θ, and value of μ are difficult to determine for the same sample.[10] Thus, there has been no viable method available to experimentally estimate the magnitude of the depolarization effect. We decided to probe this unexplored issue by studying

Chart 1. Umbrella Molecules on ITO or Au; (A−C) Three Classes of Model Compounds for SAMs Standing Upright on ITO or Gold; (D) Compound with Different Orientation on ITO (Ar = −C_6H_4−, −C_6H_4−C_6H_4− [a]
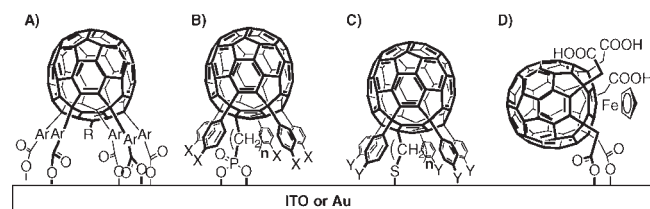
[a] R = Me, FeC_5H_5; n = 3, 4, 6; X = H, Ph, NMe_2, CF_3; Y = H, Ph).

the behavior of a series of umbrella-shaped, "pentapod" fullerene derivatives that can form a monolayer of controlled molecular density with a constant tilt angle value, standing upright by covalent bond formation between the electrode surface and either the tips of the ribs (Chart 1A) or the handle of the umbrella tube (Chart 1B,C), or standing on their sides (Chart 1D). The rigid molecular structure, the fixed molecular orientation because of the pentapod shape, and the dense and even distribution on the surface as previously elucidated by scanning tunneling microscopy (STM) and other methods[11−13] are unique for these molecules and minimize the ambiguity as to the values of n, μ, and θ in the Helmholtz equation. In addition, the flexibility of the molecular design allows us to change systematically the molecular backbone length and the electron density of the molecules by changing the n and X in Chart 1B.

We here report a quantitative demonstration of the dominant influence of the depolarization on the WF shift caused by SAM formation; that is, when the SAM of the molecules in Chart 1A−C are laid out very densely on ITO or gold, the depolarization effect due to the intermolecular charge interactions becomes so large that the WF shift becomes dependent largely on the length of the dipole. In addition we found a lack of correlation between the WF of the SAM and the ionization potential (IP) of the molecule forming the SAM. The results corroborate well what Topping formulated 80 years ago and support our previous reports on the SAMs of umbrella molecules.[11−13]

This conclusion was derived from a series of experiments including determination of a quantitative correlation between the WF of the SAM-covered surface, the dipole of the molecule, the dipole of the molecules in the SAM (denoted as depolarized dipole), IP of the molecule on the surface, the molecular orientation and a bulk surface property (water contact angle of the surface). The WF shifts were measured with an emerging new technique, photoelectron yield spectroscopy (PYS).[14]

■ EXPERIMENTAL SECTION

SAM Formation Conditions. Cleaning and pretreatment of the substrate has been known to be essential to ensure reproducibility of WF studies, in particular, for gold substrate that is highly susceptible to contamination by hydrocarbons that hinder SAM formation of thiol compounds. For the present study, we concluded that a 3 min UV/ozone pretreatment is the best choice. For ITO, we cleaned the surface with an aqueous solution of a nonionic surfactant followed by UV/ozone treatment for 3−5 min just before SAM formation. The detailed

pretreatment methods and more background information are given in the Supporting Information [SI].

Penta(organo)[60]fullerene SAMs. The SAMs of the fullerene phosphonic acid compounds were built according to the T-BAG[15] procedure. A 0.02 mM of solution of the phosphonic acid in o-dichlorobenzene (ODCB)/methanol (1:1) solution was prepared and filtered through a 0.2 μm filter prior to use. Into this solution were immersed the cleaned ITO substrates and were subsequently rinsed and sonicated in an ODCB/methanol (1:1) solution. The substrate was then heated for 24 h at 140 °C under argon atmosphere to form a covalent bond between the phosphonic acid and the ITO surface, and then sonicated in a 5% NEt$_3$ ODCB/methanol (1:1) solution, washed with ODCB and methanol, and blown dry in a stream of argon gas.

Fullerene carboxylic acid SAMs were built according to a reported procedure.[12a] ITO substrates were treated with 3-min UV/ozone cleaning and then were immersed in a 0.1 mM THF solution of the fullerene carboxylic acid compound for 3 days unless noted otherwise. The substrate was then rinsed with THF, sonicated in THF for 10 min, and dried in a stream of argon at room temperature.

The final sonication procedure for the fullerene phosphonic acid SAMs on ITO was found to be crucial to remove clusters or multilayer.[12b] The lack of the clusters or multilayers on the sample was confirmed by the PYS technique (the absence of a second ionization potential).[11]

Fullerene thiol SAMs were built under argon atmosphere using as solvent ODCB that was previously dried and degassed by freeze−thaw.[11] We allowed the molecules to form the SAM for 3 h. The substrate was then rinsed subsequently by ODCB and dichloromethane and dried in a stream of argon. This procedure produced clean SAMs without any cluster formation.

■ RESULTS AND DISCUSSION

1. Validation of the PYS Instrument. For our study of WF and IP, we employed a new technique, photoelectron yield spectroscopy (PYS).[14] The PYS technique exploits the photoelectric effect, measuring the photocurrent while irradiating the sample with monochromatic light of variable energy. The measured current is converted to photoelectron yield by a normalization procedure, which takes the photon quantum flux into account (see SI for details).

This method has an advantage over the conventional methods, ultraviolet photoelectron spectroscopy (UPS) and Kelvin probe force microscopy, for the speed of measurement, simplicity, and tolerance of a wide range of conditions. The macroscopic Kelvin probe that is also a quick method gives only the WF data, whereas the PYS method is able to determine both WF and IP simultaneously. The PYS method is applicable to conducting, semiconducting, and insulating substrates[16] covered with an organic semiconductor, placed under vacuum, and under ambient and gaseous conditions[17,18] at a variety of temperatures. Most notably, the PYS measurements can be performed next to the laboratory bench and take only minutes for each sample. However, PYS has thus far been used mainly for measurement of IPs,[11,19] and its utility for the WF measurements has not been widely recognized. Hence, we first calibrated the PYS data against those obtained by conventional methods.

WF of ITO Modified with SAMs. The groups of Armstrong and Marder determined the WFs of ITO covered with a wide variety of phosphonic acid derivatives by UPS/X-ray photoelectron spectroscopy (XPS) and by Kelvin probe.[20] For the purpose of comparison, we studied 22 phosphonic acid, carboxylic acid, sulfonic acid, and thiol derivatives that they and others

16998

dx.doi.org/10.1021/ja2067675 |J. Am. Chem. Soc. 2011, 133, 16997–17004

Chart 2. Twenty-two Compounds for SAM Formation on ITO (1−20) and Gold (21, 22)
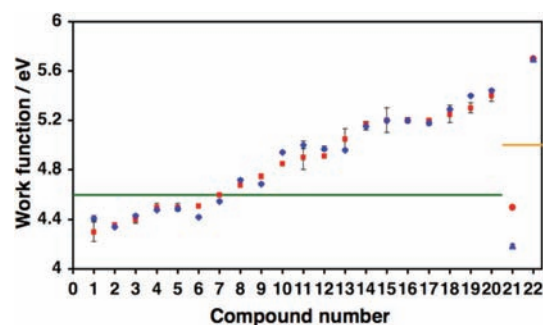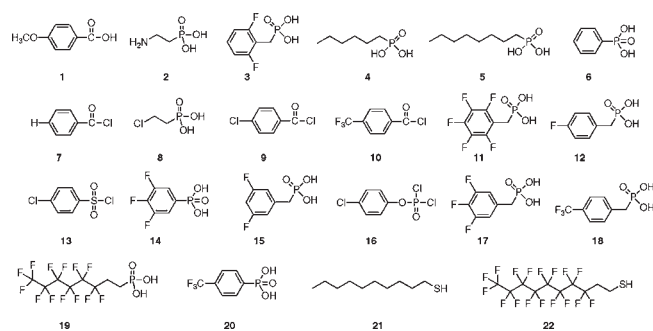
Figure 1. WFs of ITO modified with the various SAMs listed in Table 1 (compounds **1−20**) and gold modified with SAMs (compounds **21** and **22**). The PYS values are in blue and the literature values in red. Black error bars indicate the standard error. The green solid line at 4.6 eV indicates the WF of ITO treated for 5 min with UV/ozone, and the orange solid line at 5.0 eV indicates the WF of gold treated for 3 min with UV/ozone. These are the substrates used throughout the present study.

Chart 3. Three Classes of Model Compounds Used To Study the Influence of Different Parameters on the Molecular Dipole after Self-Assembly
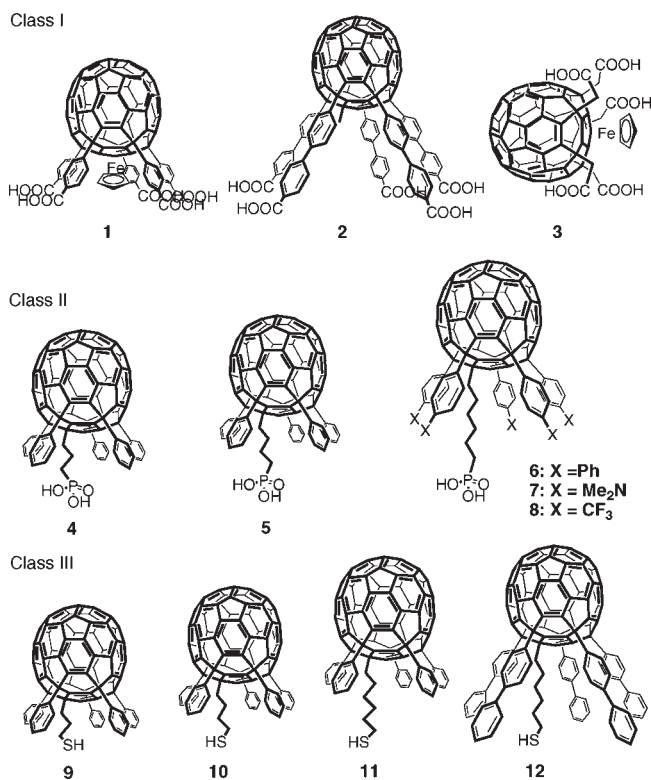

investigated. The compounds are listed in Chart 2 in order of increasing WF value.

The graph shown in Figure 1 summarizes the WF data for the 22 organic molecules in blue determined by PYS, which are shown together with the corresponding literature data in red (actual values and references are in Tables S2 and S3 [SI]). One finds that the values are roughly proportional to the expected polarity of the organic compounds. Importantly, the PYS data match very well with the literature data for a wide range of energies and compounds. Detailed information on the PYS instrument and the measurement procedure can be found in the SI.

The standard errors of the WFs for most of the phosphonic acid SAMs are particularly small (generally ±0.01 eV). One chemical reason may be the high reproducibility and high stability of the phosphonic acid SAMs on ITO.[21]

WF of Gold Modified with SAMs. In contrast to ITO, building SAMs on gold posed more problems of reproducibility, partly because of the instability of many thiol compounds in air and partly because of the above-mentioned high propensity of clean gold surfaces for hydrocarbon adsorption. The WF of a gold substrate immediately after UV/ozone cleaning for 3 min was 5.00 (±0.01) eV, whereas for untreated gold it was only 4.60 eV. It is known that coverage by organic molecules (contamination) lowers the WF of gold surfaces by as much as 0.7 eV because of the so-called "push-back" or "pillow" effect.[22] Contamination

also hinders the formation of the desired SAM with thiols, thus hampering reproducibility. For this reason, and for the general lack of reported experimental data, we list the WF data of gold only for an alkane thiol and a perfluoroalkane thiol in the rightmost part of Figure 1.

2. Selection of Model Compounds. To determine the WF and other physical parameters as a function of the diversity of molecular structures attached to an electrode (ITO and gold), we have chosen 12 penta(organo)[60]fullerenes that are classed into three different types in a way to keep certain parameters constant while others can be varied systematically. Class I includes three molecules bearing pentacarboxylic acids, Class II contains five molecules with an alkane phosphonic acid, and Class III has four molecules with an alkane thiol linker group (Chart 3).

Class I. Penta(organo)[60]fullerene Carboxylic Acids. The three umbrella molecules (**1**, **2**, and **3**) were attached to an ITO surface by the formation of COO−metal bonds. Their SAMs are known for their ability to generate only anodic (**2**) and cathodic (**1** and **3**) currents.[12a] The origin of this difference was ascribed to their vertical or lateral orientation on ITO (**1** and **2** vs **3**) as well as the presence of the ferrocene moiety that acts as a single metal atom dopant to the photoexcited fullerene moiety. The upright orientation of the penta(aryl)[60]fullerenes **1** and **2** was proven by STM[13] and other techniques, such as IR spectroscopy and XPS[23] for structurally similar molecules on various substrates. The compounds form SAMs on ITO very slowly, which made it possible to control the surface coverage (vide infra).

Our ability to install a ferrocene group (a strong electron donor)[24] allows us to probe the correlation between the WF and the IP.
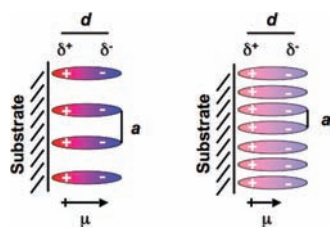
Figure 2. Schematic SAM at low surface coverage (left) and high surface coverage (right). The molecular dipoles induce an electric field in the SAM, reducing each single molecular dipole μ as indicated by the color and the length of the molecular dipole vector μ. The depolarization is displayed by the lighter color. a refers to the distance between two molecules and d to the distance between the two partial charges δ of one molecule. Note that the dipole is defined as positive if its positive pole is closest to the substrate.

The carboxylic acids **1** and **2** have different IP and molecular polarity values, although their outer molecular shapes on ITO are similar because the ferrocene moiety is hidden in the bottom cavity when **1** is attached to ITO. The lateral orientation of fullerene **3** on ITO exposes both the ferrocene and the free carboxylic acids on the top of the SAM and affects the surface properties of these SAMs. These properties were also found to be useful in studying the correlation between the WF and the IP values.[25]

Class II. Penta(organo)[60]fullerene Phosphonic Acids. The phosphonic acid side chain in fullerenes **4**−**8** quickly and strongly links the fullerene moiety on ITO.[12c] This linker allows us to change the aryl groups so that we can study the influence of the electronic properties and the molecular backbone length, both of which directly influence the molecular dipole and hence the WF. The efficacy of electronic control by the aryl group and the molecular length was suggested previously for the SAM of the same set of compounds on ITO in the study of photocurrent generation.[12c] Thus, the direction of the photocurrent upon irradiation of the SAM was influenced by the choice of electron-donating or -withdrawing aryl groups, and the efficiency of photocurrent generation was found to increase with the use of taller umbrella molecules.

Class III. Penta(organo)[60]fullerene Thiols. To attach the fullerenes on gold, we used a thiol linker instead of a phosphonic acid linker. We expected that the comparison of a SAM on ITO and on gold for the same structure of the umbrella part would provide an opportunity to study the influence of the "push-back" effects[22] of the organic molecules located on gold against the reference standard of the same molecules on ITO. The upright orientation of these fullerenes on gold was previously indicated in the study of photocurrent quantum yield measurements.[11]

3. WF Shift of Fullerene SAM-Modified ITO. The WF shift induced by SAMs is influenced by two contributions, namely, the chemical interaction between the substrate and the molecule (bond dipole) and the intrinsic dipole of the molecular backbone.[22,26] The bond dipole for thiol SAMs on gold is known to depend on the organic group attached to the sulfur atom[27] and is negligibly small for alkane thiols (<0.1 D, resulting in shifts <0.05 eV).[28] A similarly small contribution of the bond dipole was found for phosphonic acids on ITO.[29] Thus, in this study, we focused on the intrinsic dipole of the molecule, assuming that the contribution of the thiol and the phosphonic acid connecter is negligible.
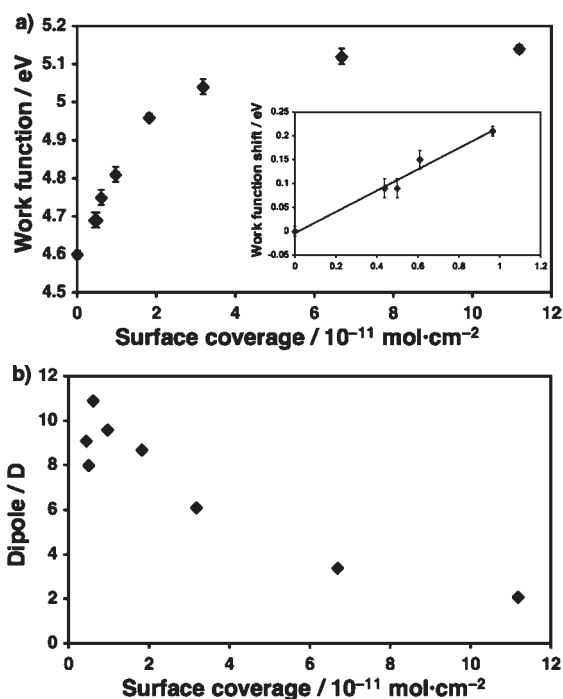

Figure 3. Correlation among surface coverage, WF, and as-measured dipole for compound **1**. (a) Surface coverage−WF relationship for pentacarboxylic acid compound **1** on ITO. Inset: The low-coverage region shows a linear dependence of WF shift on surface coverage. (b) Behavior of the molecular dipole calculated on the basis of the Helmholtz equation for different values of the surface coverage.

The molecular dipole μ_0 in the gas phase is defined as the product of two opposite charges (charge δ) and their distance apart (distance d). After SAM formation on a substrate, the charges will generate an electric field that weakens the dipole contribution of individual molecules and reduces the WF shift.[30,31] This dipole reduction is density dependent and is caused by a charge rearrangement, δ^+ and δ^-, over the molecular backbone, which is especially strong for molecules with high polarizability. Figure 2 illustrates a monolayer at low and high surface coverage showing a weakening of the dipole in the SAM at higher surface coverage. The depolarization is dependent on the distance a between two molecules (Figure 2), the polarizability α of one molecule and the molecular gas-phase dipole μ_0, as formulated by Topping in eq 2. The constant k depends only on the geometry of the periodic array of molecules ($k \cong 9.034$ for a square unit cell and $\cong 11.034$ for a triangular unit cell).

$$\mu = \mu_0/(1 + \alpha k/a^3) \qquad (2)$$

We first investigated the magnitude of the depolarization effect of our compounds by determining the correlation of the surface coverage (n) and the WF shift, from which one can calculate the depolarized dipole μ by the Helmholtz equation. The pentacarboxylic acid compound **1** was found to be particularly suitable because we can control the surface coverage by dipping time and determine it by cyclic voltammetry, as previously reported.[12a] For higher experimental accuracy, the WF value and the surface coverage were determined on the same sample. The WF shift showed a linear dependence on surface coverage for the low-coverage region as seen in the inset of Figure 3a until approximately
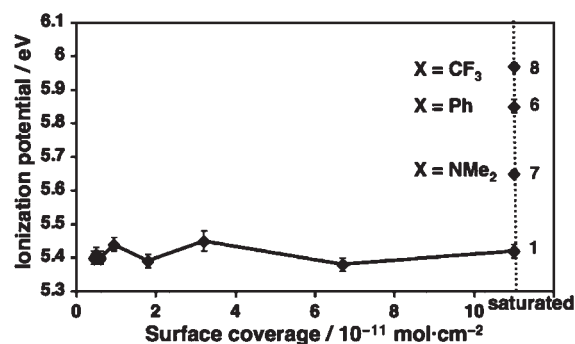
Figure 4. Surface coverage plotted against the IP for the buckyferrocene compound **1**. The IP values of the three fullerene phosphonic acid compounds **6–8** are plotted at saturated surface coverage, which was different for each molecule. Compound numbers are given for each IP value at saturated surface coverage.
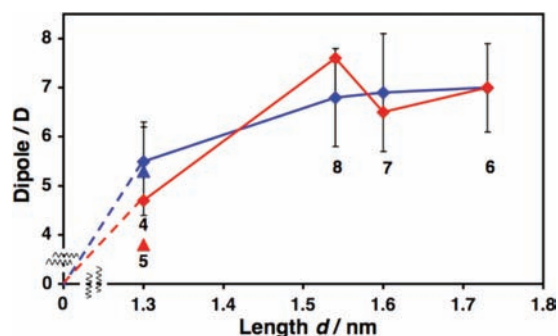

Figure 5. Relationship between the as-measured (red) and normalized (blue) molecular dipole in SAM and the length of the dipole d that we defined as the distance between the top of the C_{60} head and the end of the groups in the para position of the five X groups. The normalized dipole $\mu(n_0)$ is shown in blue and the unnormalized dipole $\mu(n)$ in red. Values for fullerene compound **5** are shown as ▲, and fullerenes **4**, **6–8** as ◆. For the raw data, see SI.
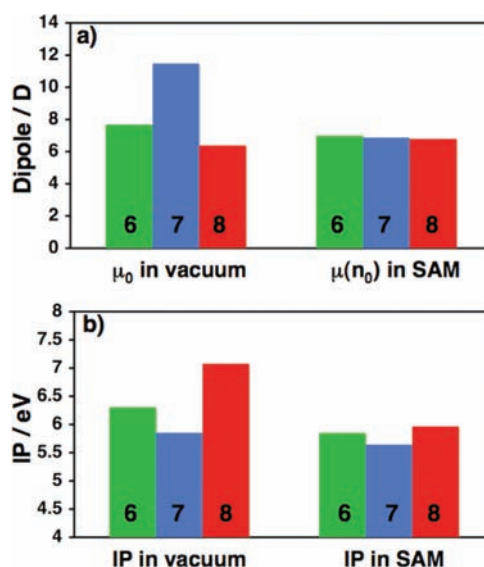
Figure 6. Comparison between calculated dipole moment and IP for a single molecule in vacuum, and experimental values. (a) Molecular dipoles. Dipoles in vacuum were calculated by the semi-empirical PM3 method that is known to be useful for a qualitative comparison of dipoles.[5] (b) IP for compound **6** (green), **7** (blue), and **8** (red) in vacuum obtained by calculations and in SAM measured by PYS. IPs were calculated by the DFT methods on a PM3-optimized geometry.

0.02 nmol/cm^2 was reached, which corresponds to an area of 8.3 nm^2 for one fullerene and translates to a mean distance of 3.3 nm from the center of one fullerene to another.

For higher surface coverage, a nonlinear dependence was observed (Figure 3a). After several days' immersion, a saturated surface coverage of 0.11 nmol/cm^2 was reached (1.5 nm^2 for one fullerene molecule), which is in good agreement with the value determined previously for this compound (see Table S4, SI, for details).[12a] From the low-coverage region, the dipole value μ_0 was determined to be 9.3 D according to the Helmholtz equation. This value is considered to be the dipole of a single molecule of pentacarboxylic acid **1** linked to ITO, because depolarization is negligible for this low-coverage area, as suggested by the linearity of the WF shift and the surface-coverage correlation in Figure 3a. The polarizability α was determined from the high-coverage region to be 7.1×10^{-28} m^3, assuming a square unit cell for the factor k in eq 2. At a coverage of higher than 20% the molecular dipole value as measured is significantly reduced, as can be seen in Figure 3b. In this figure, the molecular dipole is plotted as a function of surface coverage $\mu(n)$. This is what the Topping equation predicts and confirms the high polarizability α of these fullerene molecules, which is reasonable for this π-electron-rich compound.[32] Calculating the theoretical WF shift in the absence of depolarization from the linear fit at low surface coverage (inset Figure 3a), we obtained a value of 2.44 eV, which is 4.5 times larger than the measured WF shift of 0.54 eV. This difference of the magnitude fits well with the reported one of 5.2 times obtained by density functional theory (DFT) calculations for SAMs.[33]
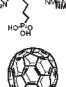
An analogous study of surface coverage dependence of the WF was performed for the taller fullerene compound **2**, and the same depolarization behavior was observed as for the pentacarboxylic acid **1** (Figure S7, SI).

Because the compounds of Classes II and III show a similar molecular structure and the same extended π-system, we used the same value of 7.1×10^{-23} m^3 for the polarizability α and therefore assumed similar depolarization behavior.

The nonlinearity of the WF shift against surface coverage has been known for some time, and Topham ascribed it to collective charge transfer between the substrate and the adsorbed molecules.[25] Therefore, we measured IPs of fullerene compound **1** on ITO at different surface-coverage values. We could not detect any change in the IP value, as seen in Figure 4

(see also Table S4, SI). In the case of charge transfer, the appearance of a lower IP value would have been expected. The IPs of the fullerene phosphonic acids **6–8** are plotted as well. Although the CF$_3$-functionalized compound **8** has a WF shift comparable to that of the buckyferrocene compound **1**, the IP values are very different. This is why we believe that Topping's depolarization theorem is best to describe the behavior of these molecules in the SAM system.

We then investigated the factors that influence the molecular dipole by systematically varying the molecular backbone length d (compounds **4–6**) or by electronic effects (δ) of the substituents in the para position of the five arene rings (fullerene compounds **6–8**) in the Class II compounds.

Table 1. Penta(organo)[60]fullerenes Self-Assembled on ITO with Corresponding WF Determined by PYS, Surface Coverage Determined by CV, IP Determined by PYS and Water Contact Angle[a]

Compound	Structure	WF (eV)	Surface coverage (mol/cm²)	Ionization potential (eV)	Water contact angle (°)
	ITO (5 min UV/ozone)	4.60 ± 0.01			7.0
4		5.15 (± 0.02)	5.1×10^{-11} ($\pm 0.6 \times 10^{-11}$)	5.93 (± 0.02)	56.7 (± 1.2)
5		5.17 (± 0.03)	6.5×10^{-11} ($\pm 1.1 \times 10^{-11}$)	5.87 (± 0.02)	69.2 (± 1.2)
6		5.24 (± 0.02)	4.0×10^{-11} ($\pm 0.4 \times 10^{-11}$)	5.85 (± 0.02)	70.0 (± 0.8)
7		5.26 (± 0.02)	4.5×10^{-11} ($\pm 0.7 \times 10^{-11}$)	5.65 (± 0.01)	62.7 (± 3.7)
8		5.14 (± 0.02)	3.1×10^{-11} ($\pm 0.3 \times 10^{-11}$)	5.97 (± 0.01)	85.5 (± 3.2)

[a] Values expressed as mean ($\pm$ standard error).
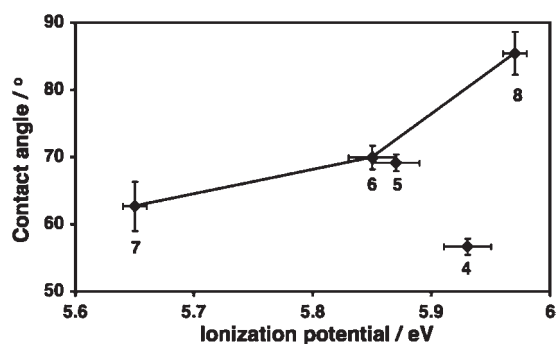
Figure 7. IPs of fullerene phosphonic acid compounds 4−8 plotted against water contact angles. Compound numbers are given for each fullerene.

These substituents are expected to influence the molecular gas-phase dipole significantly by increasing or decreasing the electron density (δ^- value) on the fullerene, which we confirmed by performing PM3 semi-empirical calculations (vide infra).

The as-measured dipoles $\mu(n)$ in the SAM (plotted as a red line in Figure 5 for the phosphonic acid compounds 4−8) against the distance d between the two partial charges δ revealed a rather random correlation between the magnitude of the dipole and its length. This randomness turns out to be because of the surface-coverage dependence of the depolarization effects formulated by Topping. Thus, we normalized the $\mu(n)$ values for one specific surface coverage, n_0, for which we took a value of 4.0×10^{-11} mol/cm²—roughly an experimental average—by the use of the correlation determined from the data in Figure 3b.

The plot of the normalized $\mu(n_0)$ against the length of the dipole d is shown as a blue line in Figure 5 and proves that $\mu(n_0)$

depends almost exclusively on d instead of the difference of the X groups in 6−8. This clearly indicates that the difference of charge distribution within the molecules is canceled by the neighboring molecules (i.e., strong depolarization effect).[32,33]

With these surprising results in hand, we calculated the dipole of a single molecule of 6−8 in vacuum to find that the Ph, Me_2N, and CF_3 substituents do affect the molecular dipole as one expects (Figure 6a, left). This difference is therefore in stark contrast to the normalized $\mu(n_0)$ in Figure 6a, right. We also calculated the IP values to find that the calculated and the experimental (vide infra) IP values show the same trend as we expect from the electron-donating and -withdrawing properties of the three substituents (Figure 6b). Thus, we reached an important conclusion that the substituents X influence the polarization within the molecule in vacuum, but the polarization on the level of individual molecules is reduced by the depolarization effect, when the molecules are densely packed in SAM, canceling the substituents effect. The IP however, is not affected, because the overall electron density remains constant before and after the self-assembling process.

4. Water Contact Angle of SAM-Covered ITO and IP. For the umbrella molecules standing upright on the substrate, the water contact angle (Table 1 and Table S5) gave us information on the electron density of the fullerene part (see Chart 1A−D).

The contact angle of ITO modified with the fullerene carboxylic acid 2 (cf. Chart 1A) was 69.0°. The 69.0° value, which is much larger than the 7.0° angle for bare ITO (Table 1, top), compares favorably with the 70° value widely observed for fullerene SAMs on zinc oxide[34] and gold[35] and hence agrees with the upright orientation of the umbrella fullerene 2 on ITO. We found that the contact angle for this compound starts to saturate at 50% coverage (60.3°) and rises slowly afterward until reaching full coverage (Figure S8, SI). This finding, together with the

Table 2. Penta(aryl)[60]fullerenes Self-Assembled on Gold with WF Values Determined by PYS and Water Contact Angles[a]

| Compound	Structure	WF value (eV)	Contact angle (°)
	Au (5 min UV/ozone)	5.00 ± 0.01	23.7 (± 1.6)
9		5.05 (± 0.01)	64.7 (± 1.6)
10		5.08 (± 0.01)	77.6 (± 1.5)
11		5.19 (± 0.01)	76.4 (± 1.3)
12		5.00 (± 0.02)	77.4 (± 1.7)

[a] Values expressed as mean (± standard error).

saturation behavior of the WF value (Figure 3), suggests that submonolayer coverage may effectively alter not only the WF,[7] but generally the physical properties of the surface.

We found a marked correlation between the contact angle and the IP of the fullerene phosphonic acids 6–8 (Figure 7). As the fullerene part of the molecules became more electron deficient in the order of 7 (X = NMe₂), 6 (Ph), and 8 (CF₃), the water contact angle increased (i.e., more hydrophobic), which is parallel to the increasing difficulty of ionization. In light of the well-known fact that fullerenes form hydrogen bonding with water,[36] we ascribe this correlation to the decreasing electronic interaction between the fullerene moiety and water because the fullerene moiety exposed to the aqueous phase becomes more electron deficient.[37] The value for the shorter fullerene compound 4 does not follow this trend but can be explained with the lower effective surface coverage and is consistent with the difference in the contact angle between the similar fullerene thiol compounds 9 and 10 on gold (Table 2).

The contact angle for the carboxylic acid compound 3, which can stand on ITO only on its side (Chart 1D), was much smaller (48.9°) than for the upright fullerenes, such as the structurally related pentacarboxylic acids 1 (61.3° ± 2.1°) and 2 (69.0° ± 0.4°; shown in Table S5, SI), as well as the phosphonic acids 6–8. We consider that the reduced contact angle is because of the exposure of the carboxylic acid units to the aqueous phase and is consistent with the side attachment of the molecule to the ITO surface.

5. WF Shift for Fullerene SAM-Modified Gold. A quantitative study using fullerene SAMs on gold was hampered by the large dipole of the metal surface that is common for metals with high IP values,[38] and caused the above-mentioned "push-back" effect. Here in our case, we consistently observed WF shifts for 9–12 on gold less by 0.3–0.6 eV than those for the structurally very similar compounds on ITO, which we ascribed to the "push-back" effect.

In light of the footprint of each compound (Figure 8), it is not surprising that the fullerene thiol 12 shows the lowest WF shift. The difference between the WF shift of 12 and that of the very
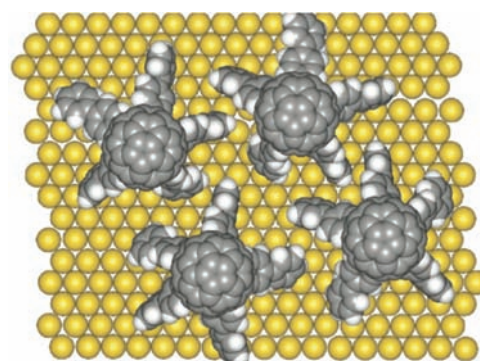
Figure 8. Fullerene thiol compound 12 on gold, as modeled after a previously reported X-ray crystal structure image. Reproduced from ref 11.

similar compound 6 on ITO is 0.64 eV, which is in good agreement with the reported reduction of the gold WF by 0.7 eV by the "push-back" effect due to the organic impurity on the metal surface.[22] The other compounds show a higher WF shift perhaps because of the longer alkyl linker that allows the fullerene molecule to be at a distance from the electron cloud of the gold surface.

This finding suggests that a consideration of the "push-back" effect of the metal surface is crucial for understanding WF shifts. This effect is negligible for ITO because the surface electrons are localized on the electronegative oxygen atoms. This idea was advanced in the study on gold and poly(3,4-ethylenedioxythiophene)/poly(styrenesulfonate) covered with conjugated organic molecules.[39]

■ CONCLUSION

In summary, the formation of a SAM of a polar compound on an electrode surface generates an electronic field through intermolecular interaction of the molecular charges, and this field makes the overall dipole of the SAM much smaller that the one expected from the simple sum of the dipole of all molecules in the SAM. In other words, the effects of intramolecular polarization are reduced when the molecules are densely packed in SAM. It has been predicted by theory and has been called depolarization effect, and here for the first time the validity of this theory is quantitatively supported by experiments. The important physical properties in surface science such as WF, IP, and water contact angles have been mutually correlated at the level of molecular structures and molecular orientations on the substrate surface. The latter issue is closely related to the problem of hierarchical control of molecules in organic electronics research.[40–42] Although the behavior of the molecules on gold initially suggested anomaly, we found that the SAMs on ITO and gold operate under the same principle which is however partially offset by the "push-back" effect of the gold surface (or other metals with high IP values). Finally, we have demonstrated the ability of the PYS technique to rapidly measure the WF of a SAM-covered substrate and the IP value of a molecule on the surface. The method will serve as a convenient tool for scientists and engineers working at the bench.

■ ASSOCIATED CONTENT

ⓢ Supporting Information. Detailed information about the PYS system, synthetic and SAM-building procedures, and

all remaining data of fullerene-modified substrates. This material is available free of charge via the Internet at http://pubs.acs.org.

■ AUTHOR INFORMATION

Corresponding Author

nakamura@chem.s.u-tokyo.ac.jp

■ REFERENCES

(1) Koch, N. *ChemPhysChem* **2007**, *8*, 1438–1455.

(2) Wu, D. G.; Ashkenasy, G.; Shvarts, D.; Ussyshkin, R. V.; Naaman, R.; Shanzer, A.; Cahen, D. *Angew. Chem., Int. Ed.* **2000**, *39*, 4496–4500.

(3) Shen, Y.; Hosseini, A. R.; Wong, M. H.; Malliaras, G. G. *ChemPhysChem* **2004**, *5*, 16–25.

(4) Topping, J. *Proc. R. Soc. London, Ser. A* **1927**, *114*, 67–72.

(5) Gershewitz, O.; Grinstein, M.; Sukenik, C. N.; Regev, K.; Ghabboun, J.; Cahen, D. *J. Phys. Chem. B* **2004**, *108*, 664–672.

(6) Peor, N.; Sfez, R.; Yitzchaik, S. *J. Am. Chem. Soc.* **2008**, *130*, 4158–4165.

(7) (a) Gozlan, N.; Tisch, U.; Haick, H. *J. Phys. Chem. C* **2008**, *112*, 12988–12992. (b) Gozlan, N.; Haick, H. *J. Phys. Chem. C* **2008**, *112*, 12599–12601.

(8) Saha, J. K.; Ahn, Y.; Kim, H.; Schatz, G. C.; Jang, J. *J. Phys. Chem. C* **2011**, *115*, 13193–13199.

(9) Evans, S. D.; Urankar, E.; Ulman, A.; Ferris, N. *J. Am. Chem. Soc.* **1991**, *113*, 4121–4131.

(10) Heimel, G.; Romaner, L.; Zojer, E.; Bredas, J.-L. *Acc. Chem. Res.* **2008**, *41*, 721–729.

(11) Matsuo, Y.; Lacher, S.; Sakamoto, A.; Matsuo, K.; Nakamura, E. *J. Phys. Chem. C* **2010**, *114*, 17741–17752.

(12) (a) Matsuo, Y.; Kanaizuka, K.; Matsuo, K.; Zhong, Y.-W.; Nakae, T.; Nakamura, E. *J. Am. Chem. Soc.* **2008**, *130*, 5016–5017. (b) Matsuo, Y.; Ichiki, T.; Radhakrishnan, S.; Guldi, D.; Nakamura, E. *J. Am. Chem. Soc.* **2010**, *132*, 6342–6348. (c) Sakamoto, A.; Matsuo, Y.; Matsuo, K.; Nakamura, E. *Chem.—Asian J.* **2009**, *4*, 1208–1212. (d) Matsuo, Y.; Ichiki, T.; Nakamura, E. *J. Am. Chem. Soc.* **2011**, *133*, 9932–9937.

(13) Chen, T.; Pan, G.-B.; Yan, H.-J.; Wan, L.-J.; Matsuo, Y.; Nakamura, E. *J. Phys. Chem. C* **2010**, *114*, 3170–3174.

(14) Riken Keiki Co., Tokyo, model AC-3, http://www.rikenkeiki.co.jp/english/.

(15) (a) Hanson, E. L.; Guo, J.; Koch, N.; Schwartz, J.; Bernasek, S. L. *J. Am. Chem. Soc.* **2005**, *127*, 10058–10062. (b) Paniagua, S. A.; Hotchkiss, P. J.; Jones, S. C.; Marder, S. R.; Mudalige, A.; Marrikar, F. S.; Pemberton, J. E.; Armstrong, N. R. *J. Phys. Chem. C* **2008**, *112*, 7809–7817.

(16) Nakayama, Y.; Machida, S.; Tsunami, D.; Kimura, Y.; Niwano, M.; Noguchi, Y.; Ishii, H. *Appl. Phys. Lett.* **2008**, *92*, 153306.

(17) Honda, M.; Kanai, K.; Komatsu, K.; Ouchi, Y.; Ishii, H.; Seki, K. *J. Appl. Phys.* **2007**, *102*, 103704.

(18) (a) Kirihata, H.; Uda, M. *Rev. Sci. Instrum.* **1981**, *52*, 68–70. (b) Koyama, A.; Kawasaki, M.; Zenba, H.; Nakajima, Y.; Yoneda, A.; Uda, M. *Nucl. Instrum. Methods Phys. Res. A* **1999**, *422*, 309–313.

(19) (a) Seki, K. *Mol. Cryst. Liq. Cryst.* **1989**, *171*, 255–270. (b) Seki, K.; Kanai, K. *Mol. Cryst. Liq. Cryst.* **2006**, *455*, 145–181. (c) Carswell, D. J.; Iredale, T. *Aust. J. Appl. Sci.* **1953**, *4*, 329–334. (d) Lyons, L. E.; Morris, G. C. *J. Chem. Soc.* **1960**, 5192–5199 and references therein. (e) Vilesov, F. I.; Terenin, A. N. *Dokl. Akad. Nauk SSSR* **1960**, *134*, 71–73. (f) Kearns, D. R.; Calvin, M. *J. Chem. Phys.* **1961**, *34*, 2026–2030. (g) Nelson, R. C. *J. Opt. Soc. Am.* **1961**, *51*, 1186–1191. (h) Harada, Y.; Inokuchi, H. *Bull. Chem. Soc. Jpn.* **1966**, *39*, 1443–1448 and references therein.

(20) (a) Armstrong, N. R.; Veneman, P. A.; Ratcliff, E.; Placencia, D.; Brumbach, M. *Acc. Chem. Res.* **2009**, *42*, 1748–1757. (b) Paniagua, S. A.; Hotchkiss, P. J.; Jones, S. C.; Marder, S. R.; Mudalige, A.; Marrikar, F. S.; Pemberton, J. E.; Armstrong, N. R. *J. Phys. Chem. C* **2008**, *112*, 7809–7817. (c) Sharma, A.; Hotchkiss, P. J.; Marder, S. R.; Kippelen, B. *J. Appl. Phys.* **2009**, *105*, 084507. (d) Sharma, A.; Haldi, A.; Hotchkiss, P. J.; Marder, S. R.; Kippelen, B. *J. Appl. Phys.* **2009**, *105*, 074511. (e) Sharma, A.; Kippelen, B.; Hotchkiss, P. J.; Marder, S. R. *Appl. Phys. Lett.* **2008**, *93*, 163308.

(21) An additional physical reason must be that the xenon lamp of the instrument is brightest at this energy range, and hence the measured currents are high. The same applies to the energy range higher than 5.2 eV where the deuterium lamp used for measurement in this energy range is brightest. In contrast, both the xenon and the deuterium lamps are intrinsically much less bright in the 5 eV range (compounds **11**−**13**), causing slightly larger errors of measurements (see Supporting Information for details).

(22) Braun, S.; Salaneck, W. R.; Fahlman, M. *Adv. Mater.* **2009**, *21*, 1450–1472.

(23) Itoh, Y.; Kim, B.; Gearba, R. I.; Tremblay, N. J.; Pindak, R.; Matsuo, Y.; Nakamura, E.; Nuckolls, C. *Chem. Mater.* **2011**, *23*, 970–975.

(24) Sawamura, M.; Kuninobu, Y.; Toganoh, M.; Matsuo, Y.; Yamanaka, M.; Nakamura, E. *J. Am. Chem. Soc.* **2002**, *124*, 9354–9355.

(25) Topham, B. J.; Kumar, M.; Soos, Z. G. *Adv. Funct. Mater.* **2011**, *21*, 1931–1940.

(26) Ishii, H.; Sugiyama, K.; Ito, E.; Seki, K. *Adv. Mater.* **1999**, *11*, 605–625.

(27) Wang, L. J.; Rangger, G. M.; Ma, Z. Y.; Li, Q. K.; Shuai, Z.; Zojer, E.; Heimel, G. *Phys. Chem. Chem. Phys.* **2010**, *12*, 4287–4290.

(28) Rusu, P. C.; Brocks, G. J. *Phys. Chem. B* **2006**, *110*, 22628–22634.

(29) Hotchkiss, P. J.; Li, H.; Paramonov, P. B.; Paniagua, S. A.; Jones, S. C.; Armstrong, N. R.; Brédas, J.-L.; Marder, S. R. *Adv. Mater.* **2009**, *21*, 4496–4501.

(30) Romaner, L.; Heimel, G.; Ambrosch-Draxl, C.; Zojer, E. *Adv. Funct. Mater.* **2008**, *18*, 3999–4006.

(31) Natan, A.; Kronik, L.; Haick, H.; Tung, R. T. *Adv. Mater.* **2007**, *19*, 4103–4117.

(32) Cornil, D.; Oliver, Y.; Geskin, V.; Cornil, J. *Adv. Funct. Mater.* **2007**, *17*, 1143–1148.

(33) Wang, L. J.; Rangger, G. M.; Romaner, L.; Heimel, G.; Bucko, T.; Ma, Z. Y.; Li, Q. K.; Shuai, Z.; Zojer, E. *Adv. Funct. Mater.* **2009**, *19*, 3766–3775.

(34) Hau, S. K.; Cheng, Y.-J.; Yip, H.-L.; Zhang, Y.; Ma, H.; Jen, A. K.-Y. *ACS Appl. Mater. Interfaces* **2010**, *2*, 1892–1902.

(35) Sahoo, R. R.; Patnaik, A. *Appl. Surf. Sci.* **2005**, *245*, 26–38.

(36) Isobe, H.; Homma, T.; Nakamura, E. *Proc. Natl. Acad. Sci. U.S.A.* **2007**, *104*, 14895–14898.

(37) (a) Andrievsky, G. V.; Klochkov, V. K.; Bordyuh, A. B.; Dovbeshko, G. I. *Chem. Phys. Lett.* **2002**, *364*, 8–17. (b) Ludwig, R.; Appelhagen, A. *Angew. Chem., Int. Ed.* **2005**, *44*, 811–815.

(38) Crispin, X.; Geskin, V.; Crispin, A.; Cornil, J.; Lazzaroni, R.; Salaneck, W. R.; Brédas, J.-L. *J. Am. Chem. Soc.* **2002**, *124*, 8131–8141.

(39) Koch, N.; Kahn, A.; Ghijsen, J.; Pireaux, J.-J.; Schwartz, J.; Johnson, R. L.; Elschner, A. *Appl. Phys. Lett.* **2003**, *82*, 70–72.

(40) (a) Cui, J.; Huang, Q. L.; Veinot, J. G. C.; Yan, H.; Marks, T. J. *Adv. Mater.* **2002**, *14*, 565–569. (b) Hsiao, C. C.; Chang, C. H.; Hung, M. C.; Yang, N. J.; Chen, S. A. *Appl. Phys. Lett.* **2005**, *86*, 223505.

(41) Bulliard, X.; Ihn, S.-G.; Yun, S.; Kim, Y.; Choi, D.; Choi, J.-Y.; Kim, M.; Sim, M.; Park, J.-H.; Choi, W.; Cho, K. *Adv. Funct. Mater.* **2010**, *20*, 4381–4387.

(42) (a) Matsuo, Y.; Sato, Y.; Niinomi, T.; Soga, I.; Tanaka, H.; Nakamura, E. *J. Am. Chem. Soc.* **2009**, *131*, 16048–16050. (b) Tsuji, H.; Mitsui, C.; Sato, Y.; Nakamura, E. *Adv. Mater.* **2009**, *21*, 3776–3779.

17004

dx.doi.org/10.1021/ja2067675 |*J. Am. Chem. Soc.* 2011, 133, 16997–17004